

SATMF Suppresses the Premature Senescence Phenotype of the ATM Loss-of-Function Mutant and Improves Its Fertility in *Arabidopsis*

Yi Zhang, Hou-Ling Wang, Yuhao Gao, Hongwei Guo and Zhonghai Li

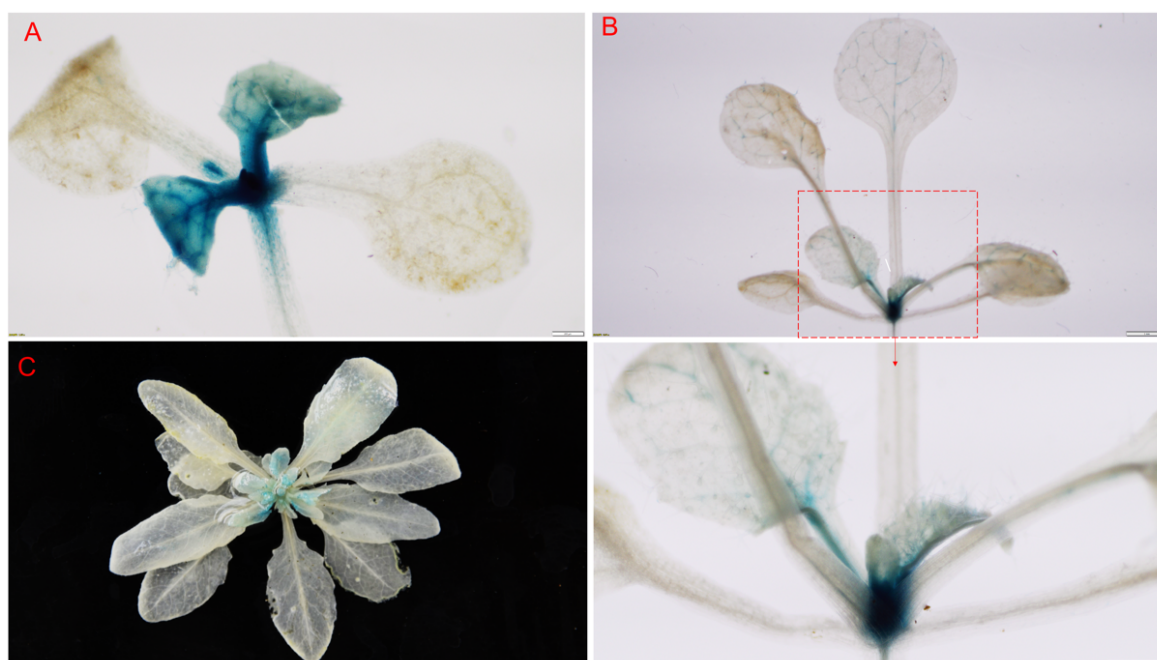


Figure S1. Histological GUS staining analysis of gene expression of ATM at different developmental stages. (A) Rosette leaves of 8-day-old seedling of *pATM-GUS/Col-0*. (B) Rosette leaves of 16-day-old plant of *pATM-GUS/Col-0*. (C) Rosette leaves of 48-day-old plant of *pATM-GUS/Col-0*.

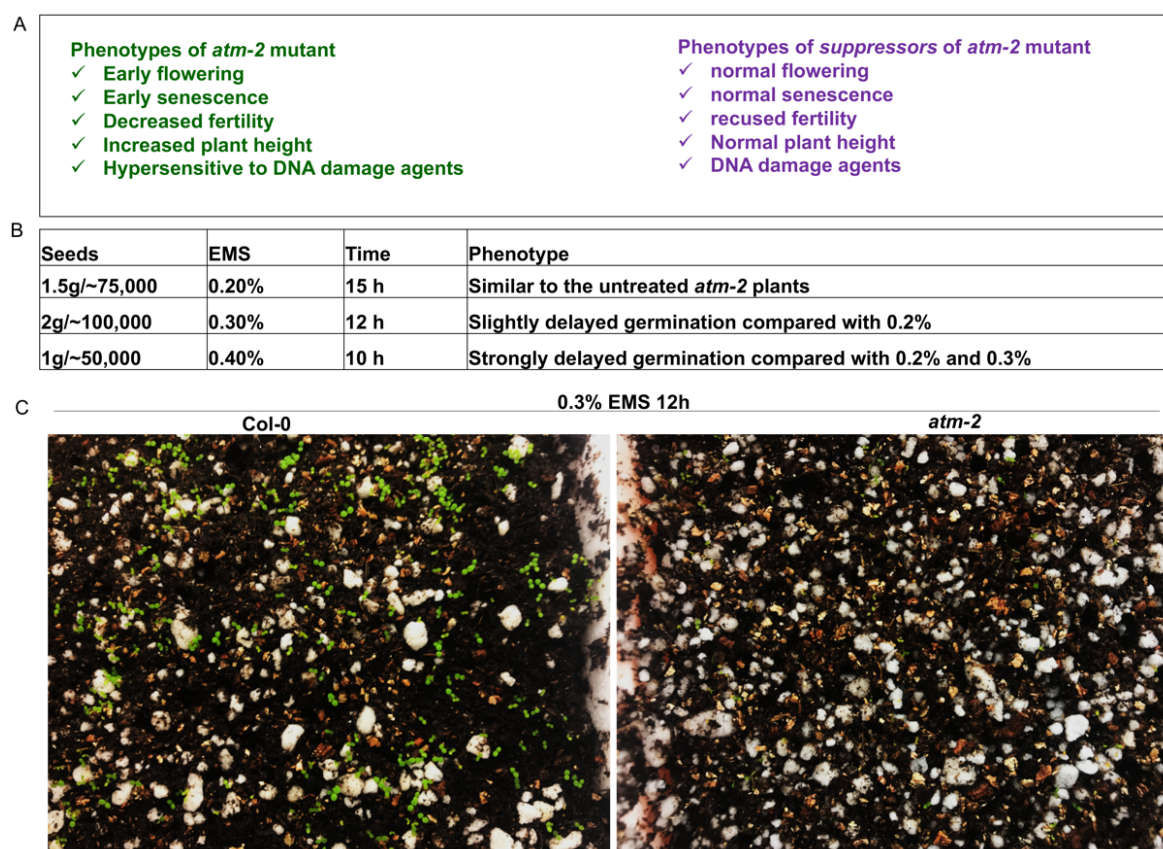


Figure S2. Screen for suppressor of *atm* mutant in fertility (*satmf*) by EMS. (A) Experimental design for screening the expected phenotypes of *satmf* mutants. (B) EMS mutagenesis of *atm-2* seeds by using different experimental conditions. (C) Seeds of *atm-2* mutant is hypersensitive to EMS in comparison to Col-0.

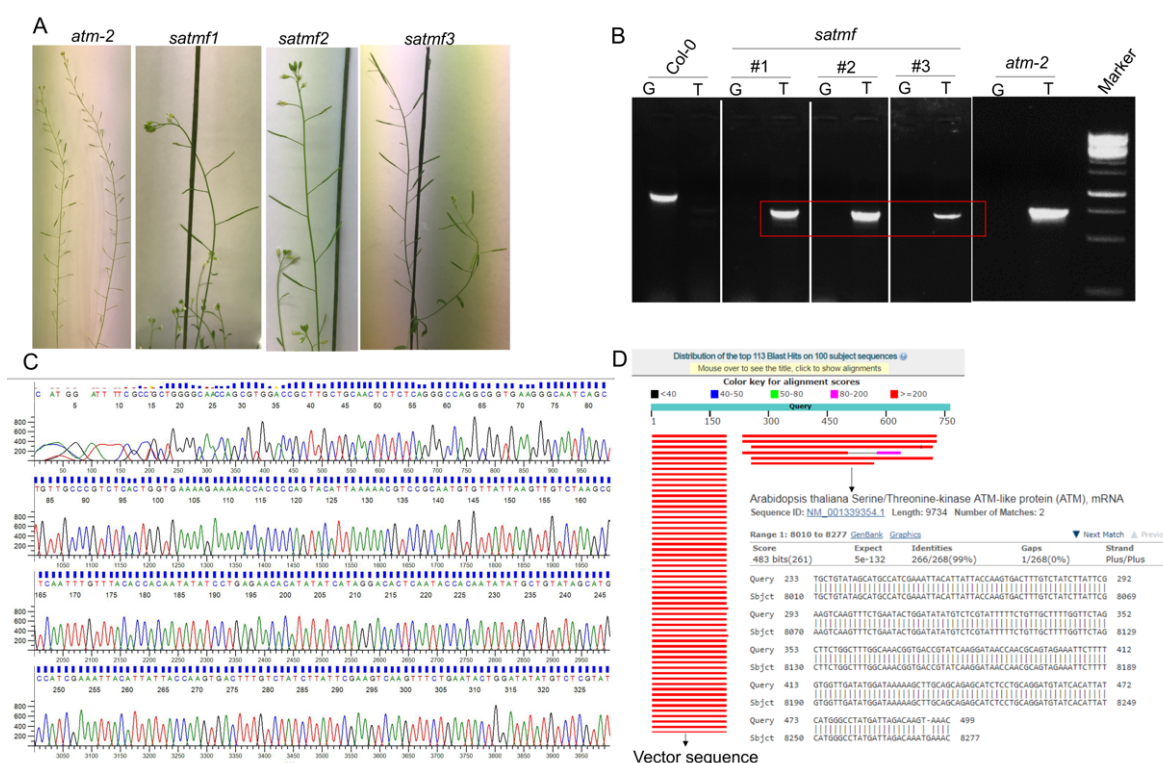


Figure S3. Molecular identification of *satmf* mutants. **(A)** Fertility of plants of Col-0, *atm-2*, *satmf1*, *satmf2* and *satmf3*. **(B)** Genotyping analysis of *atm-2*, *satmf1*, *satmf2* and *satmf3* plants. **(C)** Confirmation of the backgrounds of *satmf1*, *satmf2* and *satmf3* plants by sequencing analysis of PCR products in **(B)**. The “G” PCR reaction tests for the ability to amplify a genome region that will be present in wild type and heterozygous lines, but will not amplify in homozygous lines. The “T-DNA” PCR reaction checks for the presence of a T-DNA insertion. **(D)** BLAST analysis of the sequencing data confirms the backgrounds of *satmf* mutants.

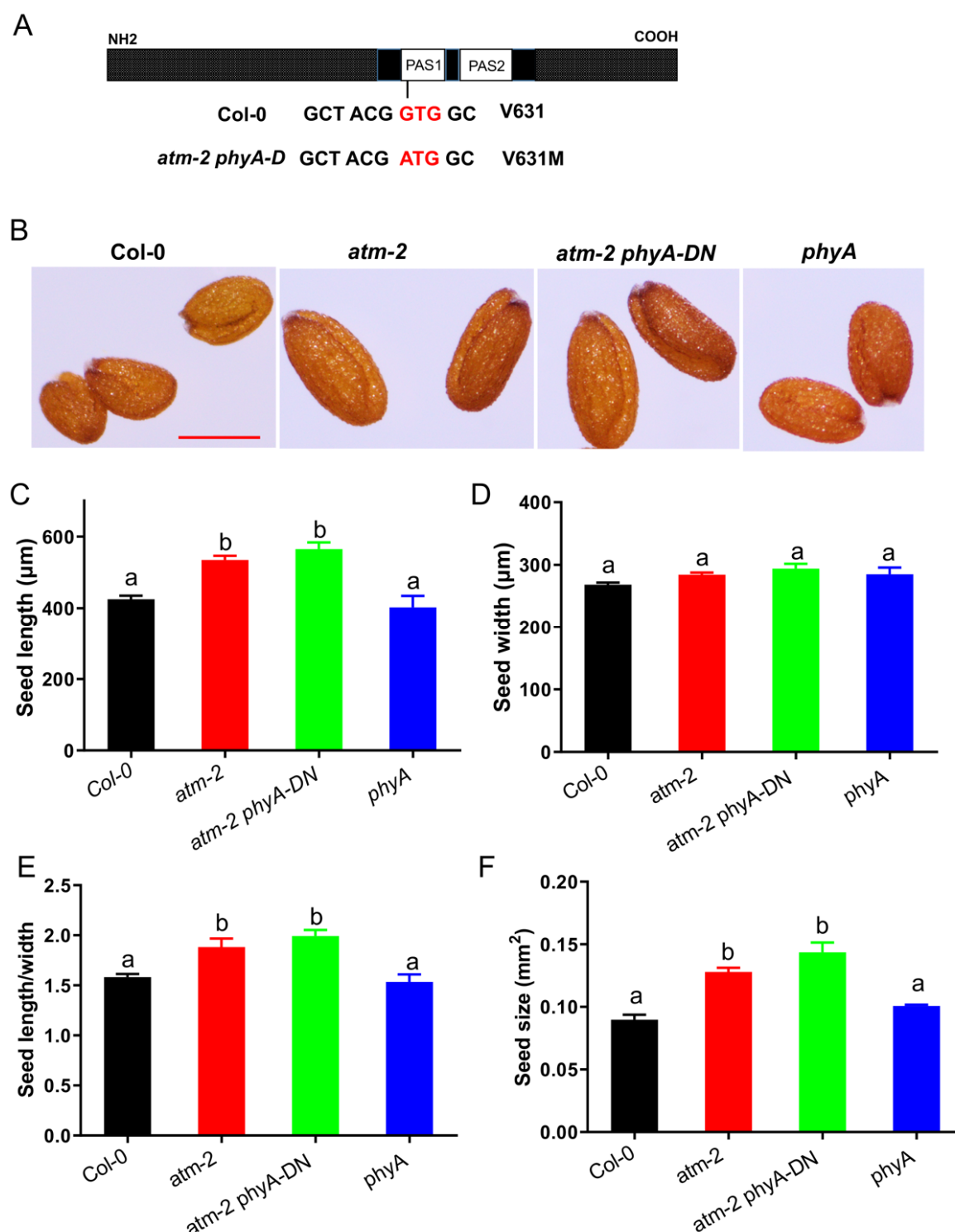


Figure S4. Identification of a dominant negative (DN) mutant of *phyA-DN*. (A) The structural features of *phyA* and the molecular lesion of the *phyA* mutation in *atm* background. There is a single amino acid residue mutation (V631M) in the translated proteins of *atm-2 phyA-DN* double mutant. (B) Mature seeds of Col-0, *atm-2*, *atm-2 phyA-DN* and *phyA* mutants. (C) Seed length, (D) seed width, (E) the ratio of length to width, and (F) seed area of mature dried seeds of Col-0, *atm-2*, *atm-2 phyA-DN* and *phyA* mutants. Values that differ at the 0.05 significance level are labeled with different letters.

Table S1. Primers used in this study.

Locus	Primer	Sequence (5' to 3')	Purpose
AT3G48190	ATM_F	ATGGTTGCTTCGAGGGATGTCC	Gene cloning
AT3G48190	ATM_R	CTAGCAAGTCCGATGCCAATTA	Gene cloning
AT3G48190	pATM_F	AGATCTTAGTCTAAAATCTATCC	Promoter cloning
AT3G48190	pATM_R	TGTGAGAGTGAGAGTAAGTGAG	Promoter cloning
AT3G48190	SALK_006953LP	ATCCATGTGGTTCAGTCTTGC	Genotyping
AT3G48190	SALK_006953RP	TTGGTATCCTGCAGAGGAAAG	Genotyping
	LB1.3	ATTTTGCCGATTTCGGAAC	Genotyping

Table S2. *Arabidopsis* genes with similarities to human disease genes (E value < 10⁻⁸⁰).

Human Disease Gene	E Value	Gene Code	Arabidopsis Hit
Darier-White, SERCA	5.9 × 10 ⁻²⁷²	AT1G10130	ARABIDOPSIS THALIANA ER-TYPE CA2+-ATPASE 3 (AtECA3)
Xeroderma Pigmentosum, D-XPD	7.2 × 10 ⁻²²⁸	AT1G03210	Putative DNA repair protein
Xeroderma pigment, B-ERCC3	9.6 × 10 ⁻²¹⁴	AT5G41360	DNA excision repair cross-complementing protein
Hyperinsulinism, ABCC8	7.1 × 10 ⁻¹⁸⁸	AT1G04120	Multidrug resistance protein
Renal tubul. acidosis, ATP6B1	1.0 × 10 ⁻¹⁸²	AT4G38510	Probable H ⁺ -transporting ATPase
HDL deficiency 1, ABCA1	2.4 × 10 ⁻¹⁸¹	AT2G41700	Putative ABC transporter
Wilson, ATP7B	7.6 × 10 ⁻¹⁸¹	AT5G44790	ATP-dependent copper transporter
Immunodeficiency, DNA Ligase 1	8.2 × 10 ⁻¹⁷²	AT1G08030	DNA ligase
Stargardt's, ABCA4	2.8 × 10 ⁻¹⁶⁸	AT2G41700	Putative ABC transporter
Ataxia telangiectasia, ATM	3.1 × 10⁻¹⁶⁸	AT3G48190	Ataxia telangiectasia mutated protein AtATM
Niemann-Pick, NPC1	1.2 × 10 ⁻¹⁶⁶	AT1G42470	Niemann-Pick C disease protein-like protein
Menkes, ATP7A	1.1 × 10 ⁻¹⁵³	AT1G63450	ATP-dependent copper transporter, putative
HNPCC, MLH1	1.5 × 10 ⁻¹⁵⁰	AT4G09140	MLH1 protein
Deafness, hereditary, MYO15	2.7 × 10 ⁻¹⁵⁰	AT2G31900	Putative unconventional myosin
Fam, cardiac myopathy, MYH7	6.5 × 10 ⁻¹⁴⁷	AT3G19960	Putative myosin heavy chain
Xeroderma Pigmentosum, F-XPF	1.4 × 10 ⁻¹⁴⁶	AT5G41150	AtRAD1 confers resistance to UV radiation. DNA repair
G6PD deficiency, G6PD	7.6 × 10 ⁻¹³⁷	AT5G40760	Glucose-6-phosphate dehydrogenase
Cystic fibrosis, ABCC7	2.3 × 10 ⁻¹³⁵	AT3G62700	MULTIDRUG RESISTANCE-ASSOCIATED PROTEIN 10
Glycerol kinase defic, GK	7.9 × 10 ⁻¹³⁵	AT1G80460	NONHOST RESISTANCE TO P. S. PHASEOLICOLA 1
HNPCC, MSH3	6.6 × 10 ⁻¹³⁴	AT4G25540	Putative DNA mismatch repair protein
HNPCC, PMS2	5.1 × 10 ⁻¹²⁸	AT4G02460	DNA mismatch repair, POSTMEIOTIC SEGREGATION 1
Zellweger, PEX1	4.1 × 10 ⁻¹²⁵	AT5G08470	Putative AAA-ATPases involved in peroxisome biogenesis
HNPCC, MSH6	9.6 × 10 ⁻¹²²	AT4G02070	G/T DNA mismatch repair enzyme
Bloom, BLM	4.4 × 10 ⁻¹⁰⁹	AT1G10930	DNA helicase ATRECQ4A involved in the maintenance of genome stability
Finnish amyloidosis, GSN	2.2 × 10 ⁻¹⁰⁷	AT5G57320	Villin 5, actin filament bundling protein
Chediak-Higashi, CHS1	5.8 × 10 ⁻⁹⁹	AT1G03070	Putative transport protein, Bax inhibitor-1 family protein
Xeroderma Pigmentosum, G-XPG	7.1 × 10 ⁻⁸⁹	AT3G28030	Non-photoreactive DNA repair, nucleotide-excision repair, response to UV-B
Bare lymphocyte, ABCB3	1.3 × 10 ⁻⁸⁴	AT5G39040	ABC transporter-like protein ABCB27, ALUMINUM SENSITIVE 1
Citrullinemia, type I, ASS	3.2 × 10 ⁻⁸³	AT4G24830	Argininosuccinate synthase-like protein involved in urea cycle
Coffin-Lowry, RPS6KA3	5.2 × 10 ⁻⁸¹	AT3G08720	Ribosomal-protein S6 kinase (ATPK19), positive regulation of translation